Title
Aquaporin deletion in mice reduces intraocular pressure and aqueous fluid production.

Journal
The Journal of general physiology, 119(6)

ISSN
0022-1295

Authors
Zhang, Duo
Vetrivel, L
Verkman, AS

Publication Date
2002-06-01

DOI
10.1085/jgp.20028597

Peer reviewed

Aquaporin Deletion in Mice Reduces Intraocular Pressure and Aqueous Fluid Production

Duo Zhang, L. Vetrivel, and A.S. Verkman

Departments of Medicine and Physiology, Cardiovascular Research Institute, University of California at San Francisco, San Francisco, CA 94143

abstract Aquaporin (AQP) water channels are expressed in the eye at sites of aqueous fluid production and outflow: AQP1 and AQP4 in nonpigmented ciliary epithelium, and AQP1 in trabecular meshwork endothelium. Novel methods were developed to compare aqueous fluid dynamics in wild-type mice versus mice lacking AQP1 and/or AQP4. Aqueous fluid production was measured by in vivo confocal microscopy after transcorneal iontophoretic introduction of fluorescein. Intraocular pressure (IOP), outflow, and anterior chamber compliance were determined from pressure measurements in response to fluid infusions using micropipettes. Aqueous fluid volume and [Cl^-] were assayed in samples withdrawn by micropipettes. In wild-type mice (CD1 genetic background, age 4–6 wk), IOP was 16.0 ± 0.4 mmHg (SE), aqueous fluid volume 7.2 ± 0.3 μl, fluid production 3.6 ± 0.2 μl/h, fluid outflow 0.36 ± 0.06 μl/h/mmHg, and compliance 0.036 ± 0.006 μl/mmHg. IOP was significantly decreased by up to 1.8 mmHg ($P < 0.002$) and fluid production by up to 0.9 μl/h in age/litter-matched mice lacking AQP1 and/or AQP4 (outbred CD1 and inbred C57/bl6 genetic backgrounds). However, AQP deletion did not significantly affect outflow, [Cl^-], volume, or compliance. These results provide evidence for the involvement of AQPs in intraocular pressure regulation by facilitating aqueous fluid secretion across the ciliary epithelium. AQP inhibition may thus provide a novel approach for the treatment of elevated IOP.

key words: water transport • AQP1 • AQP4 • anterior chamber • transgenic mice

introduction

The hydrostatic pressure of the aqueous fluid compartment of the eye, defined as intraocular pressure (IOP),* is an important index of eye physiology. Glaucoma is usually associated with elevated IOP. The principal determinants of IOP are the rate of aqueous fluid production by the ciliary epithelium and the rate of fluid drainage in the canal of Schlemm. Aqueous fluid production involves passive, near-isosmolar water transport driven by active salt transport across the ciliary epithelium. Several ion and solute transporters have been identified on pigmented and nonpigmented layers of the ciliary epithelium, which probably facilitate active solute transport. Aqueous fluid drainage is believed to involve pressure-driven bulk fluid flow in the canal of Schlemm as well as fluid movement through the sclera by seepage across the ciliary muscle and supraciliary space (Johnstone and Grant, 1973; Brandt and O'Donnell, 1999).

The transport of water across some cell plasma membranes is facilitated by aquaporin (AQP) water channels, which are small transmembrane proteins that function as passive conduits for osmotically or hydrostatically-driven water transport. AQP1 and AQP4 are expressed in nonpigmented ciliary epithelial cells in human and rat eye (Nielsen et al., 1993; Hasegawa et al., 1994; Stamer et al., 1994; Frigeri et al., 1995; Hamann et al., 1998) and have been proposed to play a role in aqueous fluid production and thus IOP regulation. Studies in transgenic mice lacking AQP1 or AQP4 have indicated that they play an important role in the urinary concentrating mechanism (Ma et al., 1997; 1998), cerebral fluid balance (Manley et al., 2000), corneal fluid balance (Thiagarajah and Verkman, 2002), hearing (Li and Verkman, 2001), and osmotically driven water transport in lung (Bai et al., 1999; Song et al., 2000a). Impaired near-isosmolar fluid absorption in kidney proximal tubules of AQP1 null mice (Schnermann et al., 1998) and impaired fluid secretion in salivary (Ma et al., 1999) and submucosal glands (Song and Verkman, 2001) of AQP5 null mice support the paradigm that AQP water channels are required for rapid, near-isosmolar fluid transport, as is thought to occur in aqueous fluid production by the ciliary epithelium. AQP1 is also expressed strongly in endothelial cells in the trabecular meshwork and canal of Schlemm (Stamer et al., 1994; Patil et al., 1997). Deletion of AQP1 in endothelial cells of the renal vasa recta impairs osmotically driven water transport and urinary

Address correspondence to Alan S. Verkman, Cardiovascular Research Institute, 1246 Health Sciences East Tower, Box 0521, University of California at San Francisco, San Francisco, CA 94143-0521. Fax: (415) 665-3847; E-mail: verkman@itsa.ucsf.edu

Abbreviations used in this paper: AQP, aquaporin; IOP, intraocular pressure.

concentrating ability (Pallone et al., 2000). However, although deletion of AQP1 in microvascular endothelia in lung (Bai et al., 1999) and pleura (Song et al., 2000b) also decreases osmotic water permeability, neither isosmolar fluid absorption nor other physiologically important processes appear to be impaired. If outflow occurs exclusively by a bulk flow mechanism, it is thus unlikely that AQP1 in endothelia in the trabecular meshwork is involved in aqueous fluid outflow. However, a recent study suggested that AQP1 may be important in trabecular endothelial volume regulation (Stamer et al., 2001), which may influence bulk fluid flow indirectly by changing the geometry of the aqueous fluid exit pathway.

The purpose of this study was to test the hypothesis that AQPs play a role in aqueous fluid dynamics and thus intraocular pressure regulation. To make quantitative comparisons in wild-type versus AQP null mice, novel methods were developed to measure the key properties of the aqueous fluid compartment including: IOP, volume, ionic composition, compliance, fluid production, and fluid outflow. Recent studies have reported IOP measurements in mice (John et al., 1997; Avila et al., 2001; Cohen and Bohr, 2001), but the other properties have not been measured. The challenges in these measurements include the small size (~7 μl aqueous fluid volume, see RESULTS) and complex geometry of the anterior chamber with little space between the corneal endothelium and lens surface, as well as the mechanical toughness of the cornea. Several strategies were evaluated and optimized in establishing the methods reported here. The new methods for measurement of the static and dynamic properties of aqueous fluid in the mouse eye should have wide applications in functional genomics using mouse models. The measurements in AQP1 and AQP4 null mice provide the first functional data concerning the role of an AQP in eye physiology, and provide evidence that AQPs are involved in IOP regulation by facilitating aqueous fluid production.

MATERIALS AND METHODS

Transgenic Mice

Transgenic knockout mice deficient in AQP1 and AQP4 were generated by targeted gene disruption in an outbred CD1 genetic background as originally described (Ma et al., 1997, 1998). The AQP1 and AQP4 null genotypes were transferred to a C57/bl6 inbred background by more than nine backcrosses. AQP1/AQP4 double knockout mice were generated by serial breedings of the single knockout mice (Song et al., 2000b). Measurements were done in matched wild-type and knockout mice of age 4–6 wk (weight 27–33 g). Mice were housed in the University of California at San Francisco animal facility, fed standard mouse chow (4% fat), and maintained on a 12 h light/12 h dark cycle. The investigators were blinded to genotype information until completion of the analysis. Protocols were approved by the University of California at San Francisco Committee on Animal Research and are in compliance with the ARVO statement for the use of animals in ophthalmic and vision research.

Mouse Preparation

Mice were generally anesthetized using ketamine (250 mg/kg intraperitoneal) alone (Burke and Potter, 1986). In some experiments, anesthesia was done using ketamine (100 mg/kg) and xylazine (9 mg/kg), or pentobarbital (50 mg/kg). The cornea was anesthetized using topical proparacaine (0.5%). Mice were immobilized using a stereotaxic device (Kopf) and body temperature was maintained at 37 ± 1°C using a heating device and rectal temperature probe. The eye was observed using a neurosurgical stereomicroscope (ZEISS) with motor-driven focus and zoom. Corneal drying was prevented using topical saline (325 mOsm to match mouse serum osmolality) that was perfused onto the corneal surface at a rate of 10 μl/min using nylon suture as a wick to prevent drop formation. The osmolality of the corneal bathing fluid remained ~325 mOsm, indicating that evaporation and hyperosmolality did not occur.

Micropipettes

IOP was measured using a fluid-filled micropipette introduced into the aqueous compartment through the cornea. A very sharp micropipette that sliced through the cornea with minimal corneal depression and trauma was found to be essential for these measurements. Initially, micropipettes were fashioned from borosilicate glass using a vertical pipette puller (model 700C; Kopf) and horizontal microforge (model MF900; Narishige). Tip outer diameters of 25–75 μm were tested. Micropipettes tips were beveled at angles of 45–60° (from pipette axis) using a rotating wheel microgrinder (model BV10; Sutter Instruments Co.), and the tip was sharpened using the microforge. Micropipettes of outer diameter 45 μm, bevel angle 50°, and short sharp tip were found to be best. However, substantially better micropipettes were prepared by simply breaking the glass pipettes, which yielded a longer bevel than that which could be fashioned with the microgrinder. Pipettes prepared in this manner were evaluated by microscopy; approximately one out of four micropipettes were judged visually to be suitable for IOP measurements. These micropipettes readily sliced through the cornea and the same micropipette was generally used for IOP and outflow measurements on >20 mice with reproducible results.

IOP

Micropipettes were introduced into the mouse cornea using a 4-axis micromanipulator (Narishige) at an angle of 45° from the vertical at a location of ~0.2 mm from the center of the cornea. Care was taken to avoid contact with the lens surface. Micropipettes were connected using short noncompliant tubing to a pressure transducer (MX860; Medex, Inc.) interfaced to a recording system (model MP100; Biopac). The circuit also permitted fluid introduction using a syringe pump (Harvard Apparatus) driving a gas-tight glass Hamilton syringe. The quality of the tubing and connections was found to be critical for accurate and stable IOP measurements, as well as elimination of small air bubbles. At the completion of each experiment the micropipette tip was withdrawn from the cornea to verify a reading of 0 mmHg. In validation studies, IOP was set at a series of specified levels (3.7–22 mmHg) by introducing a second micropipette into the anterior chamber that was connected to a fluid manometer (see Fig. 1 A).

Aqueous Fluid Outflow Dynamics

Two independent methods were used to measure aqueous fluid outflow: a continuous infusion method and a pulsed in-

fusion method; the latter method also provided information about the compliance of the aqueous fluid compartment. In the continuous infusion method, as reported for measurements in rat eye (Mermoud et al., 1996), IOP was monitored during continuous perfusion of fluid into the aqueous compartment. The rate of fluid infusion was determined empirically (see Fig. 2 A) to maintain constant IOP at a series of predetermined levels. In the pulsed infusion method, 0.1 μl infusions (rate, 20 ml/min) of fluid were made every minute during continuous IOP recording (see Fig. 3 A). From these data, volume vs. pressure (V vs. IOP) and outflow vs. pressure (dV/dt vs. IOP) curves were constructed for each eye studied (and later averaged for mice of the same genotype and genetic background) as follows: for each 0.1 μl fluid infusion, the initial and final IOPs were tabulated along with the slope [d(IOP)/dt]. Aqueous fluid volume was computed at each IOP from the measured volume at physiological IOP (see below) and the summed incremental volumes resulting from the fluid additions (after correction for outflow). The resultant V vs. IOP relation defines the compliance of the aqueous fluid compartment. Aqueous fluid outflow was computed from d(IOP)/dt and compliance: $dV/dt = dV/d(IOP) \cdot d(IOP)/dt$. Since measured outflow at physiological IOP (IOP_o) is zero as determined by the continuous and pulsed infusion methods, the measured outflow is less than total outflow at each IOP by a quantity equal to the inflow at physiological IOP. We therefore report outflow as dV/dt vs. $\Delta(IOP)$, where $\Delta(IOP) = IOP - IOP_o$.

Aqueous Fluid Production

Aqueous fluid production was measured from the kinetics of disappearance of fluorescein from anterior chamber fluid, a strategy used previously in human (Jones and Maurice, 1966; Pederson et al., 1978) and monkey (Bill, 1971) eyes. For the mouse eye, fluorescein was introduced into the anterior chamber fluid by iontophoresis (see Fig. 4 A, top) and detected by z-scanning confocal microscopy. The iontophoresis power supply consisted of an 84-V direct current supply, selectable resistors to set current, and a capacitor to attenuate current transients during switching. A cotton swab wetted with isosmolar sucrose (pH 7.3) containing 0.5 μM Na fluorescein (Sigma-Aldrich) made gentle contact with the central part of the cornea. A 0.2 mA current was passed across the cornea for 2 min. The cotton swab was connected to the negative electrode using an alligator clip and the positive electrode was connected to a needle inserted subcutaneously at the back of the neck. The cornea was then rinsed with saline and the procedure repeated using a cotton swap wetted with isosmolar sucrose (not containing fluorescein). Fluorescein concentration in the aqueous fluid was measured by z-axis scanning confocal microscopy using an apparatus described previously for measurement of airway surface liquid depth (Jayaraman et al., 2001). The apparatus consisted of a Leitz upright microscope (Diaplan) containing a Nipkow wheel coaxial-confocal module (model K2S-BIO; Technical Instruments Co.) (see Fig. 4 A, bottom). Fluorescence was detected using a standard fluorescein filter set, photomultiplier detector, and 50× long working distance objective lens (Nikon, numerical aperture 0.55, working distance 8.7 mm). The z-scan was accomplished using a stepper motor (Compumotor) driving the microscope fine focus at a scan rate of 500 μm/s. In calibration/validation experiments, confocal fluorescence z-scans were compared with aqueous fluid fluorescein concentrations measured in fluid samples drawn into microcapillaries. A series of different aqueous fluid fluorescein concentrations were generated (in separate eyes) by varying iontophoresis times from 0–3 min.

Aqueous Fluid Volume and [Cl^-]

Aqueous fluid samples were collected in empty microcapillary tubes introduced into the anterior chamber as described above. Collection of the final microliter of fluid required gentle compression of the anterior globe until the posterior surface of the cornea made complete contact with the lens. Validation measurements using wide-field fluorescence microscopy after introduction of fluorescein into the aqueous fluid indicated that >95% of aqueous fluid was withdrawn. Total fluid volume was measured by the length of the fluid column, and [Cl^-] was measured by two-color fluorescence using the indicators lucigenin and sulforhodamine 101 as described for analysis of tear fluid collected from mouse eyes (Moore et al., 2000).

Immunocytochemistry and Morphology

Mice were perfused via the aorta with 4% heparin in PBS, then with freshly prepared 4% paraformaldehyde in PBS for immunocytochemistry and 2% paraformaldehyde + 2.5% glutaraldehyde in 0.1 M sodium cacodylate buffer for light microscopy. Eyes were enucleated after immersion in the fixative solution for 2 h at room temperature after making a small cut in the cornea. Immunocytochemistry was done on frozen sections and Toluidine blue staining on plastic sections as described previously (Li et al., 2002).

RESULTS

Initial experiments confirmed the expression of AQP1 and AQP4 in nonpigmented ciliary epithelium of wild-type CD1 and C57/bl6 mice, and AQP1 in canal of Schlemm endothelia, in agreement with reports on human and rat eye. As expected for these complete knockout mice, AQP1 and AQP4 immunostaining was absent in eyes of respective null mice. Also, there were no differences in anterior chamber morphology, as assessed in stained thin plastic sections.

IOP in anesthetized mice was measured by insertion of a micropipette through the cornea into the anterior chamber (Fig. 1 A). Accurate IOP measurement required a very sharp pipette tip to avoid corneal trauma or disturbance of the lens, as well as a tight, noncomplaint fluid circuit. Fig. 1 B shows a validation study (one experiment typical of three) in which IOP was set by introduction of a second micropipette connected to a saline-filled manometer. After brief transient responses due to changes in manometer fluid heights, measured IOP agreed with the pressures set by the manometer. Subsequent IOP measurements were done using a single micropipette. As shown by the representative data in Fig. 1 C (top curve), IOP was generally stable for >30 min. IOP was decreased by mannitol or acetazolamide administration, and increased by intraperitoneal water administration, as expected (Fig. 1 C). Control studies showed good concordance in IOP measured in left versus right eyes (<1.3 mmHg difference in ~75% of mice, range 1.4–2.6 in remaining 25%). Analysis of different anesthetic regimens show on average a small decrease in IOP (1.6 ± 0.5 mmHg) using ketamine/xylazine vs. ketamine alone, and a greater

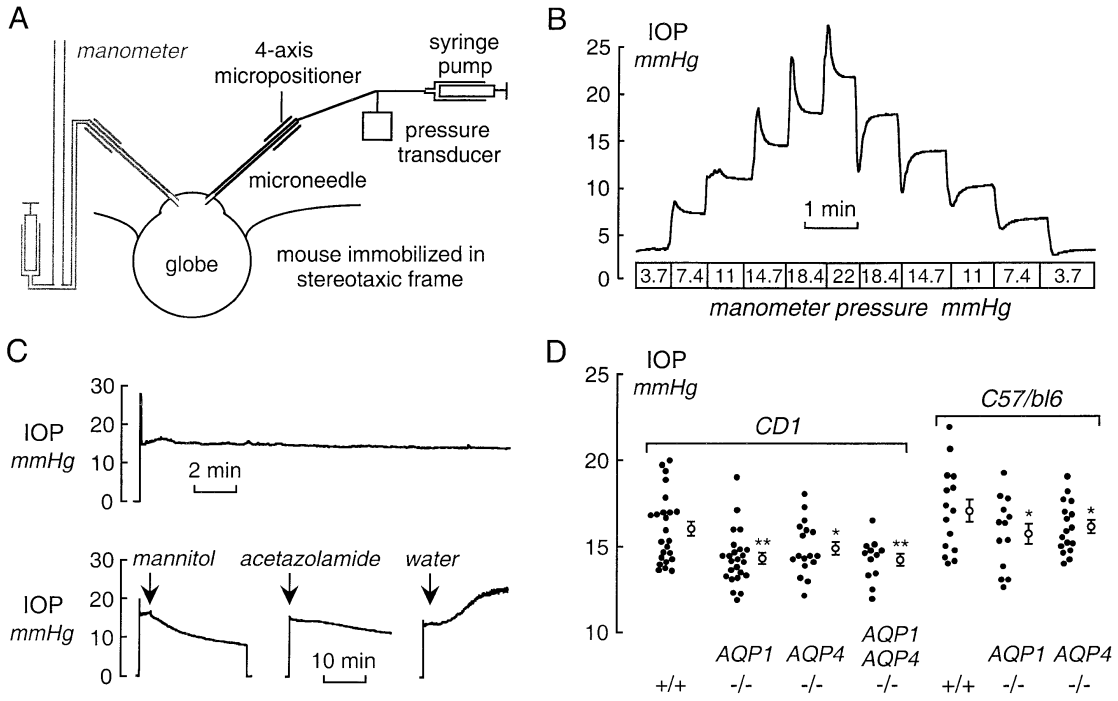

FIGURE 1. Intraocular pressure. (A) Schematic of measurement method showing the introduction of a fluid-filled micropipette into the anterior chamber through the cornea. In calibration studies, a second micropipette connected to a fluid-filled manometer was inserted (left, shown in gray). (B) Validation of IOP measurements. Measured IOP shown as a function of pressure set by manometer fluid height. (C) Time course of IOP in wild-type mice. Where indicated mice were given mannitol (20%, 2.5 g/kg), acetazolamide (8 mg/kg), or water (0.1 ml/g, intraperitoneal). (D) IOP measurements in wild-type mice, AQP1 and AQP4 null mice, and AQP1/AQP4 double knockout mice showing data in individual eyes (filled circles) and mean ± SE (open circles). *, $P < 0.05$, **, $P < 0.002$ (ANOVA).

decrease (2.6 ± 0.8 mmHg) using pentobarbital. Fig. 1 D summarizes IOP measurements on a series of wild-type mice, AQP1 null mice, AQP4 null mice, and AQP1/AQP4 double knockout mice, showing significantly reduced IOP in each of the AQP-deficient mice.

Aqueous fluid outflow was measured initially by a continuous infusion method. A micropipette connected to a pressure transducer and infusion pump was introduced into the anterior chamber. Fluid was infused continuously at rates adjusted empirically to maintain predetermined IOP values (Fig. 2 A). The inset shows a magnified view of the rate adjustments made to give a constant IOP of ~25 mmHg. Fig. 2 B shows a linear relationship between aqueous fluid outflow (μl/h) and Δ(IOP) (= IOP − IOP_o), giving an outflow rate (slope) of 0.35 ± 0.03 μl/h/mmHg, substantially less than that of 2.6 μl/h/mmHg in rat eye (Mermoud et al., 1996). Decreased outflow resistance was not seen in these studies which generally were completed within 15 min after micropipette insertion. In control studies, the kinetics of decreasing IOP was measured in four mice after elevating IOP to 30 mm Hg by continuous fluid infusion (~4 μl/h) and then suddenly stopping perfusion. In two mice, the infusion was done for 2 min and in the other two mice the infusion was done for 10 min. The rate of IOP decrease after stopping perfusion (~2 mmHg/min) was not affected by the infusion time. Experiments were also done to prove that aqueous fluid leakage did not occur at the micropipette insertion site, even at high infusion rates and elevated IOP. After infusing fluid containing fluorescein (10 μM) for 10 min at 4 μl/h in eyes of two mice (without perfusing the corneal surface), the fluorescein concentration in the fluid on the corneal surface was <10 nM, showing that no leakage occurred.

For comparative measurements in AQP null mice, a more sensitive and technically less tedious method involving pulsed fluid infusions was developed. In the pulsed infusion method, 0.1 μl fluid pulses were introduced every minute during continuous IOP recording. Each fluid addition produced a rapid increase in IOP, which is related to anterior chamber compliance, followed by a slower decline in IOP due to aqueous fluid outflow (Fig. 3 A). The rate of decline in IOP following fluid pulses was increased at higher IOPs, indicating that outflow is pressure dependent. Experiments as in Fig. 3 A were analyzed to determine the dependence of aqueous fluid volume and outflow on IOP. Fig. 3 B shows aqueous fluid volume as a function of IOP for

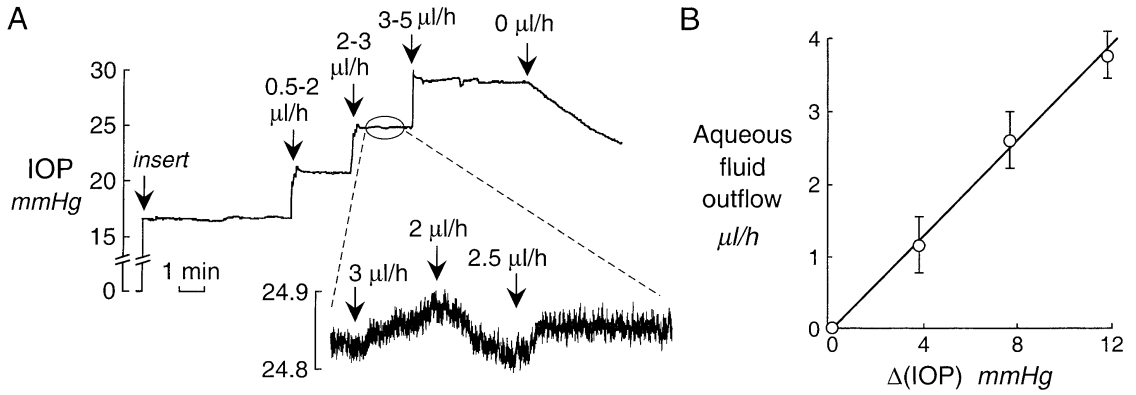

FIGURE 2. Aqueous fluid outflow by the continuous infusion method. (A) Representative experiment showing IOP recording in response to continuous fluid infusion. Fluid was infused continuously into the anterior chamber by a micropipette to obtain constant specified IOP. Infusion was transiently increased to >10 µl/h to increase IOP, followed by empirical changes by in 0.5-µl/h steps to keep IOP constant. (inset) Magnified view for setting IOP to ~25 mmHg. (B) Aqueous fluid outflow versus Δ(IOP) (IOP − IOP_o) determined from experiments as in A. Mean ± SE, n = 8 eyes.

wild-type and AQP1 null mice. Aqueous fluid volume was computed from the incremental changes in IOP as described in MATERIALS AND METHODS, using an average measured volume of 7 µl at physiological IOP (see below) for absolute volume determination. The slope of the volume versus IOP relation defines the compliance of the aqueous fluid compartment. Fig. 3 C shows aqueous fluid outflow (dV/dt, µl/h) as a function of ΔIOP. dV/dt was computed from the product of compliance, dV/d(IOP), and the rate of decline in IOP, d(IOP)/dt, following fluid pulses. Outflow rates given by the continuous (0.35 ± 0.03 µl/h/mmHg; Fig. 2 B) and pulsed (0.36 ± 0.06 µl/h/mmHg) infusion methods were in good agreement.

The approximately linear dependence of aqueous fluid outflow on IOP is in agreement with data obtained in rat (Mermoud et al., 1996) eye. Fig. 3 D (top) shows that anterior chamber compliance (slope of volume vs. IOP at IOP_o) was not affected by AQP1 deletion in mice of CD1 or C57/bl6 genetic backgrounds. Fig. 3 D (bottom) shows that aqueous fluid outflow (slope of outflow vs. Δ(IOP)) was not impaired by AQP1 deletion.

Aqueous fluid production was measured from the kinetics of fluorescein disappearance from the aqueous fluid after transcorneal iontophoresis. This approach is based on the principle that inflow and outflow are equal at IOP_o, and that outflow occurs by bulk fluid flow without sieving of the small fluorescein molecule.

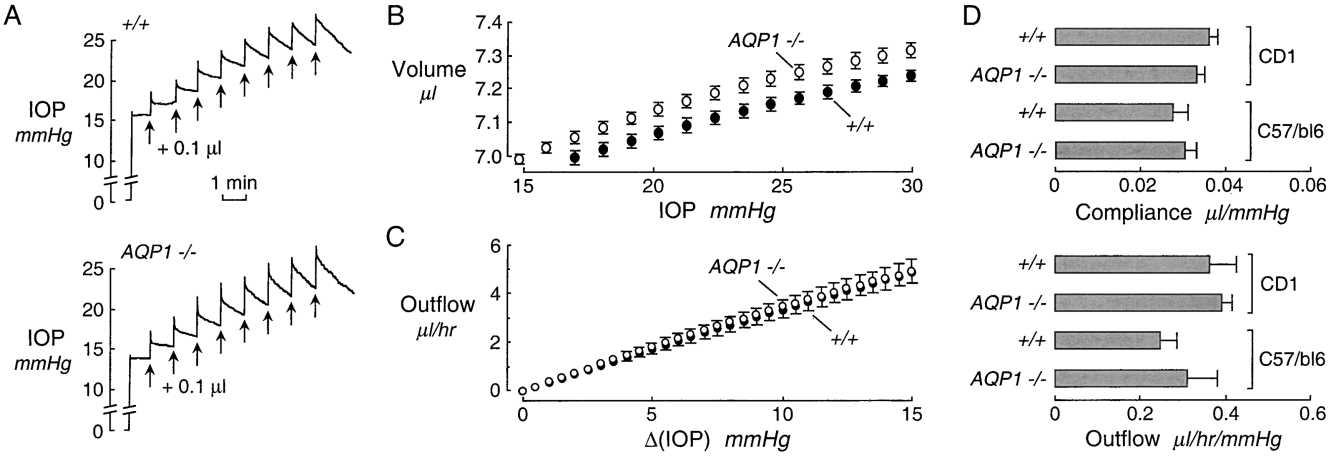

FIGURE 3. Anterior chamber compliance and aqueous fluid outflow in wild-type and AQP1 null mice measured by the pulsed infusion method. (A) Representative experiments showing continuous IOP recording in response to 0.1 µl pulsed fluid infusions every minute. The fluid infusions produced a rapid increase in IOP followed by a pressure-dependent decline due to outflow. (B) Aqueous fluid volume versus IOP for CD1 mice of indicated genotype determined from experiments as in A, defining anterior chamber compliance (mean ± SE, n = 8 eyes). See MATERIALS AND METHODS for computation procedures. (C) Δ(IOP)-dependent fluid outflow computed from rates of IOP decrease following pulsed fluid infusions. (D) Averaged anterior chamber compliance (top) and aqueous fluid outflow (bottom) for mice of indicated genotype and genetic background. Differences not significant.

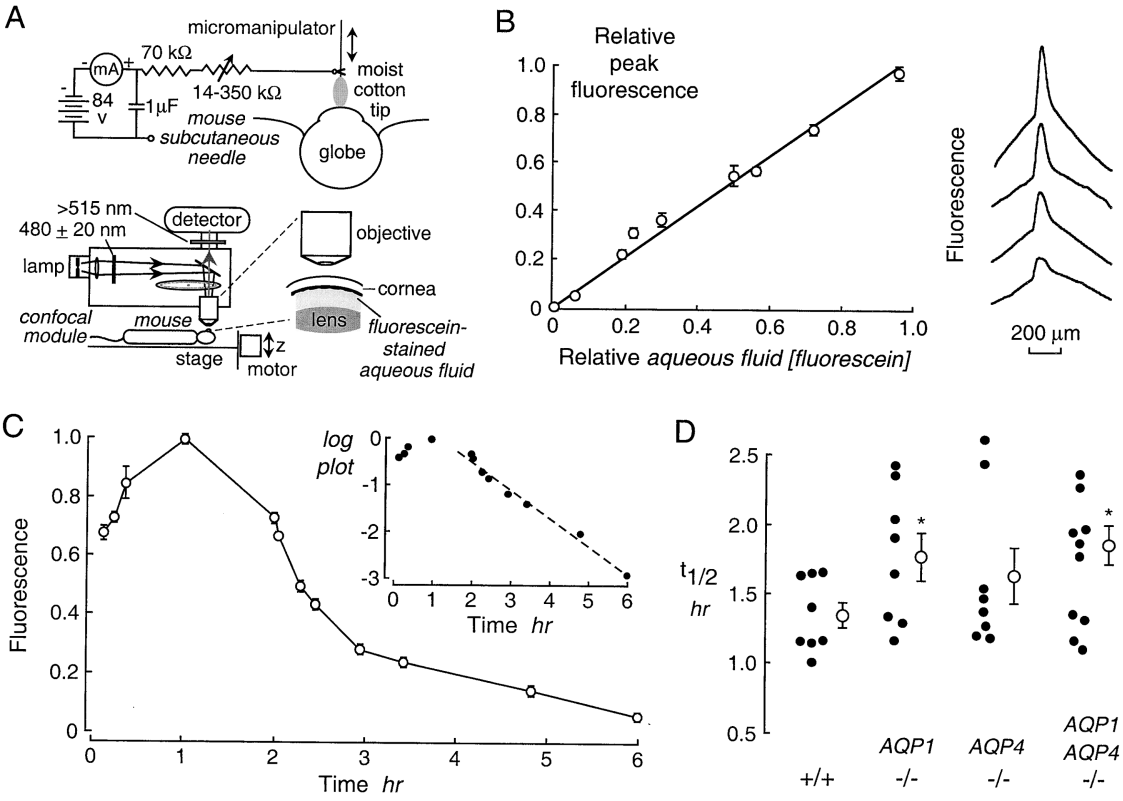

FIGURE 4. Aqueous fluid production. (A) Schematic of apparatus showing transcorneal iontophoretic introduction of fluorescein (top) and measurement of aqueous fluid fluorescein concentration by scanning confocal microscopy (bottom). (B) Linear relationship between aqueous fluid fluorescein concentration and peak height of the confocal fluorescence scan. (Left) Fluorescein concentration, measured in aqueous fluid samples withdrawn immediately after confocal microscopy, versus peak height (mean ± SE) of confocal z-scans. (Right) Representative confocal z-scans of eyes measured after iontophoresis for different times. (C) Time course of fluorescein disappearance from the anterior chamber after transcorneal iontophoretic introduction (mean ± SE). (Inset) Log plot showing approximately first-order fluorescein disappearance kinetics (dashed line) after initial equilibration period. (D) Aqueous fluid production, shown as half-times ($t_{1/2}$) for fluorescein disappearance, measured in wild-type and AQP null mice. *, $P < 0.05$ (ANOVA).

Fig. 4 A (top) shows the apparatus for iontophoresis, which consists of a cotton swap moistened with an isosmolar fluorescein-containing buffer in contact with the cornea, and a power supply delivering specified current through the cornea. Initial experiments were done to optimize the current, iontophoresis time, and fluorescein concentration to introduce readily measurable quantities of fluorescein into the aqueous fluid without damage to the cornea and with minimal fluorescein remaining in the cornea. A short iontophoresis time (2 min) and a small current (0.2 mA) effectively loaded the anterior chamber fluid with fluorescein, probably because of the relatively thin mouse cornea (~120 μm thickness) compared with corneas from humans and larger animals (>500 μm). After rinsing the cornea, electrical current was passed through the cornea for an additional 2 min (without fluorescein) to drive most of the remaining fluorescein out of the corneal stroma into the aqueous fluid.

After testing various approaches to measure aqueous fluid fluorescein concentration (wide-field microscopy at low and high numerical aperture, micropipette sampling), we used in vivo z-scanning fluorescence confocal microscopy with a 50× long working distance air objective lens (Fig. 4 A, bottom). Confocal microscopy permitted measurement of fluorescein concentration in the aqueous fluid just beneath the corneal endothelium with minimal geometric and scattering effects. To validate the confocal measurement approach, z-scans were obtained for a series of eyes in which different amounts of fluorescein were introduced by varying iontophoresis durations from 0 to 3 min. The peak heights deduced by confocal microscopy (Fig. 4 B, right) were compared with fluorescein concentrations measured in microcapillary samples of aqueous fluid obtained just after confocal microscopy. Fig. 4 B (left) shows excellent linearity between results of scanning confocal microscopy and relative fluorescein concentration. The peak height of the fluorescence z-scan thus provides a quantitative index of aqueous fluid fluorescein concentration. To show that the peak height represents fluorescein in the aqueous fluid rather than in the cornea

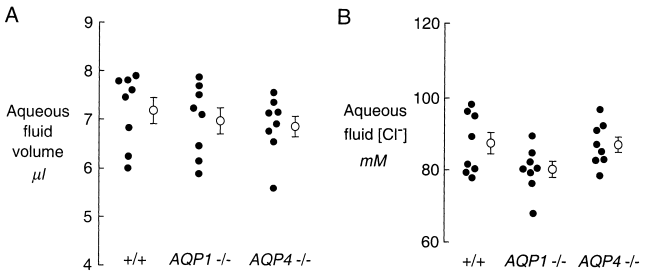

FIGURE 5. Aqueous fluid volume and [Cl^-]. (A) Aqueous fluid volumes, obtained by microcapillary sampling, measured on wild-type and AQP null mice. Data from individual eyes (filled circles) and mean ± SE (open circles) shown. (B) [Cl^-] measured in the aqueous fluid samples. Differences not significant.

or other fixed structures, confocal microscopy was done just after washout of the aqueous fluid by dual micropipette perfusion (Thiagarajah and Verkman, 2002) of the anterior chamber (30 μl/min for 3 min) with fluorescein-free solution. After washout, peak height was < 4% of that before washout.

Fig. 4 C shows the time course of aqueous fluid fluorescein concentration, deduced by z-scanning confocal microscopy, for measurements on eight eyes from wild-type mice. To minimize exposure to anesthetics, measurements on individual mice were made just after iontophoresis and at no more than two subsequent times. There was an initial increase in aqueous fluid fluorescein concentration, probably representing diffusion of any fluorescein remaining in the corneal stroma, followed by a slower decline representing bulk fluid outflow (which equals fluid inflow at IOP_o). From the plot of log(fluorescence) versus time (Fig. 4 C, inset), the $t_{1/2}$ for fluorescein disappearance was ~1.3 h The aqueous inflow rate computed from $t_{1/2}$ and aqueous fluid volume was 3.6 ± 0.2 μl/h. Based on the time course data in Fig. 4 C, confocal microscopy in subsequent comparative measurements was done just after iontophoresis and at 1.5 and 3 h.

Fig. 4 D summarizes $t_{1/2}$ for experiments on 8–10 eyes in each group. Aqueous fluid production was significantly slowed (increased $t_{1/2}$) by deletion of AQP1 alone, or AQP1 and AQP4 together.

Last, the total fluid volume of the aqueous compartment was measured by direct microcapillary withdrawal of fluid. Care was taken to ensure nearly quantitative removal of fluid, as verified by fluorescence measurements in eyes in which the aqueous compartment was stained with fluorescein. Fig. 5 A summarizes aqueous fluid volumes, which were quite consistent from mouse to mouse. Aqueous fluid volume did not differ significantly in AQP1 or AQP4 null mice from that in wild-type mice. Because of the low anterior chamber compliance (0.036 μl/mmHg), it is not possible to detect possible decreases in aqueous fluid volume in AQP null mice (~0.07 μl for 2 mmHg change in IOP).

The aqueous fluid samples obtained for volume measurements were assayed for [Cl^-] using a two-color microfluorimetry method developed previously for [Cl^-] measurements in submicroliter quantities of tear fluid. Fig. 5 B shows similar [Cl^-] in aqueous fluid from wild-type and AQP1 or AQP4 null mice.

DISCUSSION

Experiments were done to investigate whether AQP water channels are involved in intraocular pressure regulation and aqueous fluid dynamics. As discussed in the INTRODUCTION, the involvement of AQPs in aqueous fluid dynamics has been proposed, without functional evidence, from their specific localization in cells involved in aqueous fluid handling. Comparative measurements were done in wild-type mice and mice lacking AQP1 and/or AQP4, an approach that has been informative in defining the role of AQP1 and AQP4 in renal (Ma et al., 1997, 1998), lung (Bai et al., 1999), gastrointestinal (Ma et al., 2001), and neuromuscular (Manley et al., 2000) physiology. AQP1 null mice are grossly phenotypically normal, but manifest distinct abnormalities when stressed by water deprivation, high fat diet, or certain types of pain. AQP4 null mice also appear normal but are hearing impaired and show reduced brain swelling in response to acute injury. Measurements of the static and dynamic properties of the aqueous fluid in the mouse eye were quite challenging and required a series of technical developments. Our results establish the rates of aqueous fluid inflow and outflow in the mouse eye, as well as the static aqueous fluid pressure, volume, and compliance. Comparative measurements in AQP null mice showed significant reductions in IOP and aqueous fluid production, without differences in aqueous fluid outflow, volume, [Cl^-], or anterior chamber compliance.

IOP was measured using sharp micropipettes based on the original method described by John et al. (1997). As detailed in the MATERIALS AND METHODS section, a number of modifications in micropipette design, corneal penetration procedures, and pressure measurements were made to give reproducible IOP values in our laboratory. The micropipette method gave stable IOP for >30 min and did not cause leak of aqueous fluid. Advantages of the relatively large (~50 μm) micropipettes used here include the ability to record rapid changes in IOP and to introduce fluids into the aqueous compartment. Recently, a servo-null method was reported for measurement of IOP in mouse eyes, which utilizes a small, ~5-μm diameter micropipette filled with a 3 M KCl solution (Avila et al., 2001). The servo-null method also permits continuous recording of IOP, but the small pipette tip precludes the introduction of fluid into the

aqueous compartment. The IOP measured here in CD1 mice (16.0 ± 0.4 mmHg) and C57/bl6 mice (17.1 ± 0.6 mmHg) is in agreement with IOP measured by John et al. (1997) for different mouse strains (11.1–19.3 mmHg) (Savinova et al., 2001) and with the servo-null data (17.8 ± 0.4 mmHg) (Avila et al., 2001).

Aqueous fluid inflow was determined using a fluorescein disappearance method as originally developed for measurements in the human eye. The principle of this method is that aqueous fluid inflow and outflow are equal in the steady-state at physiological IOP, and that fluorescein removal occurs by bulk fluid outflow. Fluorescein was efficiently introduced into the aqueous fluid by iontophoresis without trauma to the eye. Initial attempts to introduce fluorescein by corneal puncture with small micropipettes were inconsistent because of fluid leak after micropipette removal, even when attempting to seal the leak using glue or opthalmic suture. Fluorescein concentration in the aqueous fluid was assayed noninvasively by scanning confocal microscopy. Control studies showed that the fluorescence signal provided a linear, quantitative measure of fluorescein concentration in the aqueous fluid. A full fluorescein disappearance curve, constructed from measurements on multiple mice, was used to select two times on the exponentially decreasing phase of the disappearance curve for comparative studies of wild-type versus AQP null mice. Because of limitations in repeated or long-term anesthesia in mice, it was not possible to measure a full fluorescein time course in individual mice for a three-compartment analysis of fluorescein disappearance. The two-point analysis method used here assumes that the kinetics of fluorescein exchange between the aqueous fluid and cellular/interstitial compartment is similar in wild-type and AQP null mice.

Analysis of the kinetics of fluorescein disappearance in wild-type CD1 mice gave an aqueous fluid inflow rate of 3.6 ± 0.2 μl/h, substantially lower than that of 210 μl/h in rabbit eye (Becker and Constant, 1956; Ruben et al., 1985), 60–105 μl/h in monkey eye (Bill, 1971; Sperber and Bill, 1984), 150 μl/h in human eye (Jones and Maurice, 1966), and 21 μl/h in rat eye (Mermoud et al., 1996). Aqueous fluid production was significantly reduced in mice lacking AQP1 alone or AQP1/AQP4 together. The impairment in AQP null mice probably results from decreased water permeability in nonpigmented cells in the ciliary epithelium where the bulk of aqueous fluid is likely to flow.

Aqueous fluid outflow was measured from changes in IOP in response to continuous and pulsed fluid infusions into the anterior chamber. Based on similar measurements in rat eye (Mermoud et al., 1996), aqueous fluid outflow was estimated directly from empirically determined rates of continuous infusion, giving constant IOP at a series of predetermined levels. It is assumed in this method that at constant IOP fluid infusion and outflow are equal in the steady-state. A second method, which provided quantitative information about both static compliance and aqueous fluid outflow, was the measurement of IOP in response to serial infusions of small (0.1 μl) fluid volumes. Data from both methods indicated an approximately linear increase in aqueous fluid outflow with Δ(IOP) with a slope of ~0.36 μl/h/mmHg. Outflow was not impaired in AQP1 null mice, which is consistent with bulk fluid flow that is predicted not to involve water-selective AQPs. The reason(s) for AQP1 expression in endothelia of the trabecular meshwork and canal of Schlemm remain unclear, but our results provide evidence that they are not related to aqueous fluid outflow. AQP1 appears to be present in numerous capillary beds (Nielsen et al., 1993; Hasegawa et al., 1994) without apparent physiological significance (Bai et al., 1999; Moore et al., 2000; Song et al., 2000b).

In summary, quantitative methods have been established to measure the static and dynamic properties of aqueous fluid in mouse eye, and we report the first data on aqueous fluid production, outflow, compliance and volume. These methods should facilitate mechanistic analysis of the roles of various membrane transporters on IOP regulation using specific inhibitors or transgenic mice. AQP1 and/or AQP4 deletion produced coordinate decreases in IOP and aqueous fluid production. However, the clinical significance of the modest reduction in IOP in AQP-deficient mice remains uncertain. Application of IOP-reducing agents, such as carbonic anhydrase inhibitors, reduce IOP by only a few mmHg in normal human eyes. Further studies are indicated to determine the role of AQP deletion in mouse models of increased IOP and glaucoma, and when available, to determine effects of acute AQP inhibition by specific blockers.

We thank Dr. Simon John for helpful advice on IOP measurements in the initial stages of our study, and Liman Qian for transgenic mouse breeding and genotype analysis.

This work was supported by grants EY13574, DK35124, HL59198, HL60288, and EB00415 from the National Institutes of Health and a grant from the Cystic Fibrosis Foundation.

Submitted: 18 March 2002
Revised: 19 April 2002
Accepted: 22 April 2002

REFERENCES

Avila, M.Y., D.A. Carré, R.A. Stone, and M.M. Civan. 2001. Reliable measurement of mouse intraocular pressure by a servo-null micropipette system. *Invest. Ophthalmol. Vis. Sci.* 42:1841–1846.

Bai, C., N. Fukuda, Y. Song, T. Ma, M.A. Matthay, and A.S. Verkman. 1999. Lung fluid transport in aquaporin-1 and aquaporin-4 knockout mice. *J. Clin. Invest.* 103:555–561.

Becker, B., and M.A. Constant. 1956. The facility of aqueous outflow. A comparison of tonography and perfusion measurements in vivo and in vitro. *Arch. Opthalmol.* 55:305–312.

Bill, A. 1971. Aqueous human dynamics in monkeys. *Exp. Eye Res.* 11:195–206.

Brandt, J.D., and M.E. O'Donnell. 1999. How does the trabecular meshwork regulate outflow? Clues from the vascular endothelium. *J. Glaucoma.* 8:328–339.

Burke, J.A., and D.E. Potter. 1986. The ocular effects of xylazine in rabbits, cats and monkeys. *J. Ocul. Pharmacol.* 2:9–21.

Cohen, B.E., and D.R. Bohr. 2001. Measurement of intraocular pressure in awake mice. *Invest. Ophthalmol. Vis. Sci.* 42:2560–2562.

Frigeri, A., M. Gropper, C.W. Turck, and A.S. Verkman. 1995. Immunolocalization of the mercurial-insensitive water channel and glycerol intrinsic protein in epithelial cell plasma membranes. *Proc. Natl. Acad. Sci. USA.* 92:4328–4331.

Hamann, S., T. Zeuthen, M. La Cour, E.A. Nagelhus, O.P. Ottersen, P. Agre, and S. Nielsen. 1998. Aquaporins in complex tissues: distribution of aquaporins 1-5 in human and rat eye. *Am. J. Physiol.* 274:C1332–C1345.

Hasegawa, H., S.C. Lian, W.B. Finkbeiner, and A.S. Verkman. 1994. Extrarenal tissue distribution of CHIP28 water channels by *in situ* hybridization and antibody staining. *Am. J. Physiol.* 266:C893–C903.

Jayaraman, S., Y. Song, L. Vetrivel, L. Shankar, and A.S. Verkman. 2001. Non-invasive in vivo fluorescence measurement of airway surface liquid depth, salt concentration, and pH. *J. Clin. Invest.* 107:317–324.

John, S.W.M., J.R. Hagaman, T.E. MacTaggart, P. Li, and O. Smithes. 1997. Intraocular pressure in inbred mouse strains. *Invest. Opthalmol. Vis. Sci.* 38:249–253.

Johnstone, M.A., and W.M. Grant. 1973. Pressure-dependent change in structures of the aqueous outflow system of human and monkey eyes. *Am. J. Ophthalmol.* 75:365–383.

Jones, R.F., and D.M. Maurice. 1966. New methods for measuring the rate of aqueous flow in man with fluorescein. *Exp. Eye Res.* 5:208–220.

Li, J., and A.S. Verkman. 2001. Impaired hearing in mice lacking aquaporin-4 water channels. *J. Biol. Chem.* 276:31233–31237.

Li, J., R.V. Patil, and A.S. Verkman. 2002. Mildly impaired retinal function in transgenic mice lacking aquaporin-4 water channels. *Invest. Opthalmol. Vis. Sci.* 43:573–579.

Ma, T., Y. Song, A. Gillespie, E.J. Carlson, C.J. Epstein, and A.S. Verkman. 1999. Defective secretion of saliva in transgenic mice lacking aquaporin-5 water channels. *J. Biol. Chem.* 274:20071–20074.

Ma, T., K.S. Wang, J.A. Bastidas, and A.S. Verkman. 2001. Defective dietary fat processing in transgenic mice lacking aquaporin-1 water channels. *Am. J. Physiol.* 280:C126–C134.

Ma, T., B. Yang, A. Gillespie, E.J. Carlson, C.J. Epstein, and A.S. Verkman. 1997. Generation and phenotype of a transgenic knock-out mouse lacking the mercurial-insensitive water channel aquaporin-4. *J. Clin. Invest.* 100:957–962.

Ma, T., B. Yang, A. Gillespie, E.J. Carlson, C.J. Epstein, and A.S. Verkman. 1998. Severely impaired urinary concentrating ability in transgenic mice lacking aquaporin-1 water channels. *J. Biol. Chem.* 273:4296–4299.

Manley, G.T., M. Fujimura, T. Ma, N. Noshita, F. Filiz, A. Bollen, P. Chan, and A.S. Verkman. 2000. Aquaporin-4 deletion in mice reduces brain edema following acute water intoxication and ischemic stroke. *Nat. Med.* 6:159–163.

Mermoud, A., G. Baeveldt, D.S. Minckler, J.A. Prata, and N.A. Rao. 1996. Aqueous humor dynamics in rats. *Graefe's Arch. Clin. Exp. Opthalmol.* 234:S198–S203.

Moore, M., T. Ma, B. Yang, and A.S. Verkman. 2000. Tear secretion by lacrimal glands in transgenic mice lacking water channels AQP1, AQP3, AQP4 and AQP5. *Exp. Eye Res.* 70:557–562.

Nielsen, S., B.L. Smith, E.I. Christensen, and P. Agre. 1993. Distribution of the aquaporin CHIP in secretory and resorptive epithelia and capillary endothelia. *Proc. Natl. Acad. Sci. USA.* 90:7275–7279.

Pallone, T.L., A. Edwards, T. Ma, E. Silldorff, and A.S. Verkman. 2000. Requirement of aquaporin-1 for NaCl driven water transport across descending vasa recta. *J. Clin. Invest.* 105:215–222.

Patil, R.V., I. Saito, X. Yang, and M.B. Wax. 1997. Expression of aquaporins in the rat ocular tissue. *Exp. Eye Res.* 64:203–239.

Pederson, J.E., D.E. Gaaterland, and H.M. MacLellan. 1978. Accuracy of aqueous human flow determination by fluorophotometry. *Invest. Opthalmol. Vis. Sci.* 17:190–195.

Ruben, J.B., R.A. Moses, and W.J. Grodzki. 1985. Perfusion outflow facility in the rabbit eye: stabilization by EACA. *Invest. Opthalmol. Vis. Sci.* 26:153–158.

Savinova, O.V., F. Sugiyama, J.E. Martin, S.I. Tomarev, B.J. Paigen, R.S. Smith, and S.W. John. 2001. Intraocular pressure in genetically distinct mice: an update and strain survey. *BMC Genet.* 2:12–20.

Schnermann, J., J. Chou, T. Ma, M.A. Knepper, and A.S. Verkman. 1998. Defective proximal tubule reabsorption in transgenic aquaporin-1 null mice. *Proc. Natl. Acad. Sci. USA.* 95:9660–9664.

Song, Y., and A.S. Verkman. 2001. Aquaporin-5 dependent fluid secretion in airway submucosal glands. *J. Biol. Chem.* 276:41288–41292.

Song, Y., T. Ma, M.A. Matthay, and A.S. Verkman. 2000a. Role of aquaporin-4 in airspace-to-capillary water permeability in intact mouse lung measured by a novel gravimetric method. *J. Gen. Physiol.* 115:17–27.

Song, Y., B. Yang, M.A. Matthay, T. Ma, and A.S. Verkman. 2000b. Role of aquaporin water channels in pleural fluid dynamics. *Am. J. Physiol.* 279:C1744–C1750.

Sperber, G.O., and A. Bill. 1984. A method for near-continuous determination of aqueous humor flow; effects of anesthetics, temperature and indomethacin. *Exp. Eye Res.* 39:435–453.

Stamer, W.D., K. Peppel, M.E. O'Donnell, B.C. Roberts, F. Wu, and D.S. Epstein. 2001. Expression of aquaporin-1 in human trabecular meshwork cells: role in resting cell volume. *Invest. Ophthalmol. Vis. Sci.* 42:1803–1811.

Stamer, W.D., R.W. Snyder, B.L. Smith, P. Agre, and J.W. Regan. 1994. Localization of aquaporin CHIP in the human eye: implications in the pathogenesis of glaucoma and other disorders of ocular fluid balance. *Invest. Ophthalmol. Vis. Sci.* 35:3867–3872.

Thiagarajah, J.R., and A.S. Verkman. 2002. Aquaporin deletion in mice reduces corneal water permeability and delays restoration of transparency after swelling. *J. Biol. Chem.* In press.